

Tuning and optical study of the ΓX and ΓL photonic pseudogaps in opals

P. D. García, J. F. Galisteo-López, and C. López^{a)}

*Instituto de Ciencia de Materiales de Madrid (CSIC), C/ Sor Juana Inés de la Cruz 3,
28049 Madrid, Spain*

(Received 17 June 2005; accepted 22 September 2005; published online 10 November 2005)

In this letter we demonstrate a method to tune and optically investigate the two highest-symmetry pseudogaps in artificial opals which occur at the L and X points of the Brillouin zone and correspond to propagation along the (111) and (100) crystallographic directions, respectively. In particular we show that in artificial opals the gap at the X point, which is closed for bare opals, can be opened by controlled infiltration with a high refractive index material such as ZnO. To prove this we take advantage of the fact that, in artificial opals grown by the vertical deposition method, regions with both (100) and (111) orientations of the face centered cubic lattice occur naturally. © 2005 American Institute of Physics. [DOI: 10.1063/1.2132068]

The interaction between electromagnetic radiation and matter shows interesting properties in the so-called photonic crystals.¹ These are composite materials presenting a periodic dielectric constant for which multiple scattering of incident light results in dispersion relations organized in bands separated by frequency intervals in which there are no available states and light propagation is forbidden. Such intervals may be strongly directional, in which case they are known as pseudogaps. A great variety of structures present properties as one, two, or three-dimensional (1D, 2D, or 3D) photonic crystals. Among 3D photonic crystals, synthetic opals² stand out for their low cost of fabrication and their easy manipulation. Growth methods for such structures, known as self-assembly methods, rely on the natural tendency that some inorganic (SiO₂) or organic [polystyrene (PS), poly(methylmethacrylate) (PMMA)] microspheres have to form ordered face cubic centered structures. Among such methods³ natural sedimentation⁴ and vertical deposition⁵ are the most popular approaches.

One of the most interesting properties of photonic crystals is that they allow to modify the photon density of states. The latter is determined by the band structure which may be tailored by means of variations in the refractive index contrast and topology for a given symmetry. Although for artificial opals the symmetry is fixed by the growth process, the band structure can be modified, to a certain extent, by means of a controlled infiltration with high dielectric constant materials carrying out what can be called band gap engineering.^{6,7} Knowledge of the photonic band structure of synthetic opals and the possible modifications attainable by engineering through infiltration is desirable in order to exploit their potential in applications for light steering such as super refractive devices. For artificial opals at low frequencies ($a/\lambda < 1$, where a is the lattice parameter and λ the wavelength of light in vacuum), pseudogaps appear for propagation along different crystallographic directions. The width of such pseudogaps is mostly dictated by the magnitude of the Fourier component (in the expansion of the dielectric function) associated with the reciprocal lattice vector G corresponding to such direction.⁸ Therefore, for a fixed symmetry, the interaction and, hence, pseudogap width may be manipulated modifying the refractive index distribution and volume fraction.⁹

In this work we demonstrate a method to tune the two highest-symmetry pseudogaps in artificial opals occurring in the reciprocal space directions ΓL and ΓX which correspond to crystallographic orientations (111) and (100), respectively. In particular the ΓX gap, closed for bare opals, can be opened. As a playground we use areas of the opal that present either of these orientations which naturally appear in artificial opals grown by vertical deposition. They can be identified by the symmetry of the arrangement of spheres in the surface of the sample. Areas of hexagonal (square) arrangement of spheres correspond to $\{111\}$ ($\{100\}$) planes. While several high-symmetry directions have been studied in bulk artificial opals by inspecting cleft edges,¹⁰ they are difficult to cut, the available areas are small, difficult to locate, orientate and align with the spectroscopic experimental setup. While thin film opals grown by vertical deposition have almost always their $\{111\}$ planes parallel to the substrate, in some cases naturally occurring (100) oriented regions appear as already reported by several authors.^{11,12} This occurs mostly in the initial stages of growth.

The samples used were grown using polystyrene (PS) spheres 503 nm in diameter (3% polydispersity) synthesized by a previously published method.¹³ ZnO infiltration of the sample was carried out with a modified metal-organic chemical vapour deposition method¹⁴ by using a metal-organic precursor which allows a fine control of shell thickness (of a few nm). In order to remove PS spheres to obtain a ZnO inverted opal, the sample was calcinated at 450 °C for 2 hours. A Fourier transform infrared spectrometer (Bruker IFS-66/S) was used to record the optical reflectance of the samples at normal incidence in a wide spectral range. A microscope attached to the spectrometer with a $\times 4$ objective featuring a 0.1 numerical aperture ($\pm 5.7^\circ$ angular aperture) was used to focus and collect the light. We have performed all measurements in adjacent regions with square and hexagonal planes in areas of 9 and 11 layers of thickness, respectively. The thickness was estimated from Fabry-Perot oscillations present in the spectra on either side of the Bragg peak. Optical microscopy (Fig. 1) and scanning electron microscopy (Fig. 2) were used to characterize the morphology of the samples. Optical microscopy was performed with the same objective used for optical measurements. In order to perform the scanning electron microscopy inspection, the samples were coated with a thin gold film as customary.

^{a)}Electronic mail: cefe@icmm.csic.es

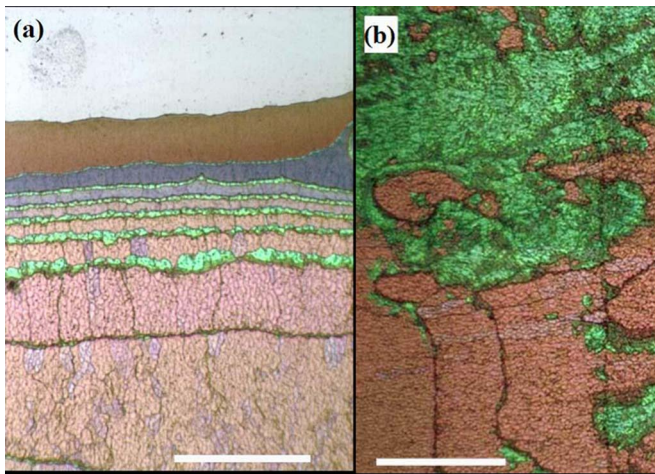


FIG. 1. (Color online) Optical microscopy images showing regions with different morphology. (a) Initial stages of sample growth at the top of the sample. (b) Wide region presenting green and pink colors. Scale bar is $375 \mu\text{m}$ in both cases.

Optical microscopy images show sample regions presenting different appearance. At the early stages [top of the sample in Fig. 1(a)] growth takes place by the formation of terraces of increasing thickness with steps more or less parallel to the (horizontal) meniscus line. As the sample thickness increases, the color of the terraces varies from brown (1 layer) to pink (>7 layers). At the boundaries between terraces bright green colors are observed. Even when the sample has reached a stationary thickness [Fig. 1(b)], some regions present fairly wide ($>1 \text{ mm}^2$) green and pink colored areas coexisting.

A closer inspection of the above mentioned regions by means of electron microscopy provides structural information at a more local level. Figure 2(a) shows the first stages of growth of the sample presented in Fig. 1(a). In the image, sample thickness grows from one (left) to three (right) layers.

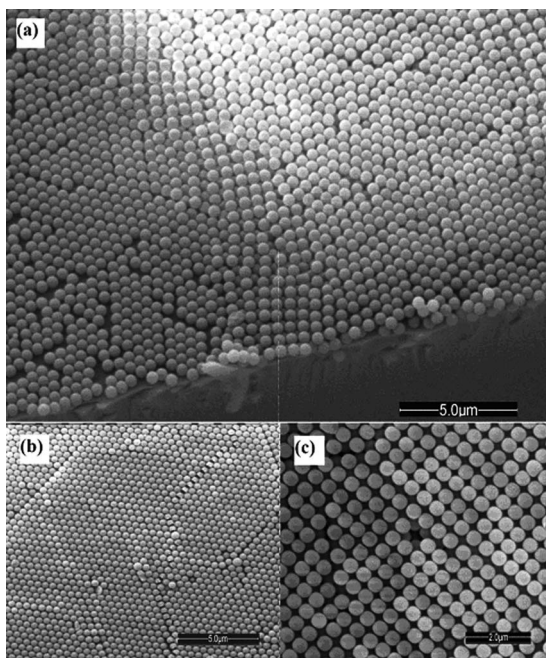


FIG. 2. SEM images: (a) Initial stages of growth at the top of the sample, (b) hexagonal areas corresponding to pink regions in Fig. 1(b), and (c) square areas corresponding to green regions in Fig. 1(b).

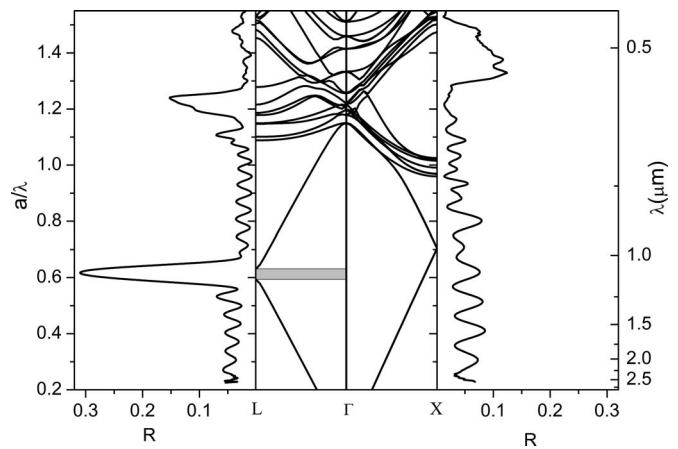


FIG. 3. Left (right) panel shows reflectance collected in hexagonal (square) regions of a bare opal. Central panel shows the corresponding photonic bands.

Alternation between square and hexagonally arranged planes takes place, and accounts for the different colors observed. Where square arrangements appear green colors are observed, while hexagonal ones account for the brown-pink areas. Such alternation has been previously observed in similar samples¹⁵ and has been accounted for by invoking an optimal filling of the meniscus region where the ordering of the sample takes place.¹⁶ Electron microscopy inspection of large pink [Fig. 2(b)] and green [Fig. 2(c)] areas, as those in Fig. 1(b), confirms their (111) and (100) orientation. The existence of wide regions with (100) orientation amid the prevailing (111) constitutes a perfect playground to carry out the study of the pseudogap associated with both propagation directions due to their width and thickness.

For the bare opal, the hexagonal area presents (Fig. 3, left panel) a strong reflectance peak (1160 nm) which corresponds to the calculated¹⁷ pseudogap taking place along the ΓL direction. The high energy response ($a/\lambda > 1$) of these regions presents a maximum of intensity for $\lambda = 583 \text{ nm}$, which accounts for the pink color. Square areas do not present a reflectance peak at low energies (Fig. 3, right panel). This is due to the fact that the pseudogap is closed in the ΓX direction for this low refractive index contrast, although a feature in Fabry-Perot oscillations appears in the spectra in the same position ($a/\lambda = 0.7$) where the two sets of degenerate energy bands meet. The green color of this region is accounted for by the reflectance peak around $\lambda = 517 \text{ nm}$ in the high energy range. Incidentally we wish to say that the high energy response of synthetic opals has been studied before^{18–20} and is known to be a signature of the high quality of the samples. This rules out misgivings about not having a reflectance feature due to low quality of the inspected region.

The degree of infiltration of the opal can be assessed by comparing the spectral position of the first order Bragg from (111) facets with the calculated pseudo-gap in the ΓL direction.²¹ Increasing the pore filling fraction with a high index material affects differently the X and L pseudogaps spectral width. A study performed by means of band structure calculations shows that, for the case of the inverted structure, for which the largest modification of the X pseudogap is expected, a 35% filling is optimal for achieving a maximum spectral width for both pseudogaps. Figure 4 presents the optical response of an opal with such filling fraction.

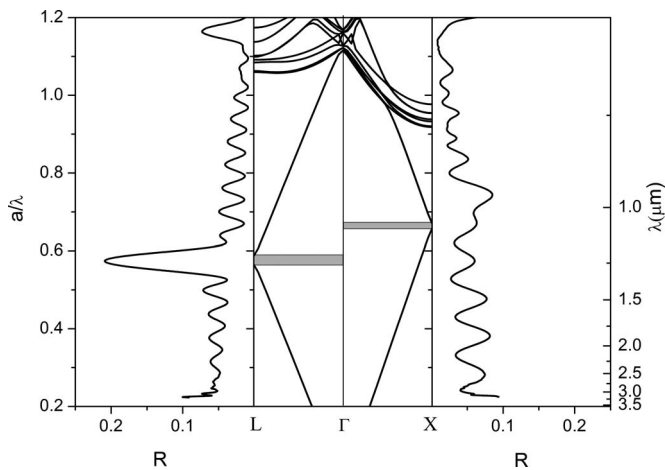


FIG. 4. Left (right) panel shows reflectance collected in hexagonal (square) regions of a PS-ZnO opal. Central panel shows the corresponding photonic bands.

For the infiltrated opal (Fig. 4) a reflectance peak appears in the spectrum from the (100) oriented region due to the opening of a pseudogap in the ΓX direction (0.011 broad in a/λ units). The calculated pseudogap width in the ΓL direction is 0.025. This difference in breadth explains the different intensity in the peaks corresponding to the two different crystal orientations. That the reflectance peak corresponding to the ΓX direction appears in a spectral position slightly blueshifted compared to the pseudogap predicted by the band diagram in this direction could be explained by finite size effects, previously reported for the ΓL direction^{22,23} but not studied for the ΓX direction yet.

After the calcination process and opal inversion, reflectance spectra have been recorded for both crystal orientations (Fig. 5). For the ΓX direction (right panel) reflectance spectra shows a strong (18%) reflectance peak with, approximately, the same intensity as that of the first-order maximum along the ΓL direction. This fact is again accounted for by pseudogap widths in either direction in accordance with the calculated bands (0.049 in the ΓX direction and 0.037 in the ΓL direction).

It is also worth mentioning that the high quality of the samples used allows the study of optical features in the high energy regime. In this spectral region interplay between sev-

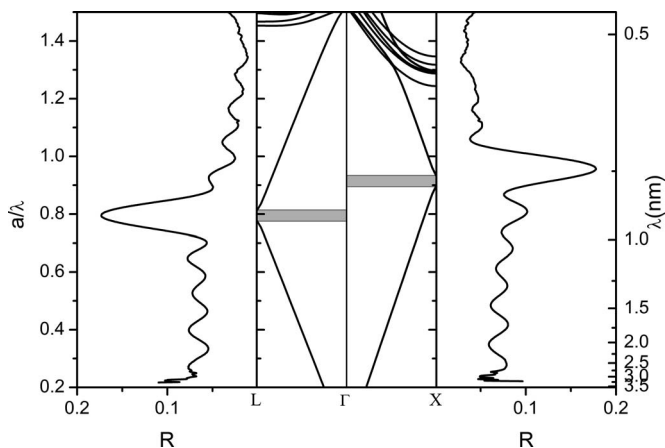


FIG. 5. Left (right) panel shows reflectance collected in hexagonal (square) regions of a ZnO inverted opal. Central panel shows the corresponding photonic bands.

eral families of planes strongly modifies the bandstructure of the system and frequency intervals where flat, dispersionless bands develop (e.g., Fig. 3). The group velocity associated with these bands becomes small,⁸ increasing the interaction time between electromagnetic radiation and the materials forming the crystal. One may benefit from such low group velocity modes to explore enhancement of ZnO emission which could eventually open up routes to fabricate efficient light emitting devices in the UV part of the spectrum.

In summary, in this work we have performed an optical study of the pseudogap occurring in the ΓX and ΓL directions, profiting for this purpose from naturally occurring (100) and (111) oriented growth in artificial opals that show facets with square and hexagonal symmetry arrangements, respectively. We have demonstrated its dependence on dielectric contrast. We have thus successfully shown an application of bandgap engineering to open an otherwise closed pseudogap which will be very interesting to future refractive applications. The ability to control the growth of such square layers would redound to the benefit of photonic engineering as it would eliminate a major constrain in artificial opal growth. Work towards this direction is currently being performed.

This work has been partially financed by the EU network of excellence FP6-511616 PHOREMOST; the ESF COST action P11 and the Spanish MEC through MAT-2003-01237 project.

¹E. Yablonovitch, Phys. Rev. Lett. **58**, 2059 (1987); S. John, *ibid.* **58**, 2486 (1987).

²V. N. Astratov, Nuovo Cimento D **17**, 1349 (1995).

³C. López, Adv. Mater. (Weinheim, Ger.) **15**, 1679 (2003).

⁴R. Mayoral, J. Requena, J. S. Moya, C. López, A. Cintas, H. Miguez, F. Meseguer, L. Vázquez, M. Holgado, and A. Blanco, Adv. Mater. (Weinheim, Ger.) **9**, 257 (1997).

⁵P. Jiang, J. F. Bertone, K. S. Hwang, and V. L. Colvin, Chem. Mater. **11**, 2131 (1999).

⁶H. Miguez, E. Chomski, F. García-Santamaría, M. Ibisate, S. John, C. López, F. Meseguer, J. P. Mondia, G. A. Ozin, O. Toader, and H. M. van Driel, Adv. Mater. (Weinheim, Ger.) **13**, 1634 (2001).

⁷F. García-Santamaría, M. Ibisate, I. Rodríguez, F. Meseguer, and C. López, Adv. Mater. (Weinheim, Ger.) **15**, 10 (2003).

⁸K. Sakoda, *Optical Properties of Photonic Crystals* (Springer, Berlin, 2001).

⁹I. Tarhan and G. H. Watson, Phys. Rev. B **54**, 7593 (1996).

¹⁰E. Palacios-Lidón, A. Blanco, M. Ibisate, F. Meseguer, C. López, and J. Sánchez-Dehesa, Appl. Phys. Lett. **81**, 4925 (2002).

¹¹A. Y. Vlasov, Xiang-Zheng Bo, J. C. Sturm, and D. J. Norris, Nature (London) **414**, 289 (2001).

¹²Q. B. Meng, C. H. Fu, Y. Einaga, Z. Z. Gu, A. Fujishima, and O. Sato, Chem. Mater. **14**, 83 (2002).

¹³J. W. Goodwin, J. Hearn, C. C. Ho, and R. H. Ottewill, Colloid Polym. Sci. **252**, 464 (1974).

¹⁴B. H. Juárez, P. D. García, D. Golmayo, A. Blanco, and C. López, Adv. Mater. (Weinheim, Ger.) (to be published) (early view DOI: 10.1002/adma.200500569).

¹⁵N. D. Denkov, O. Velez, P. Kralchevski, I. Ivanov, H. Yoshimura, and K. Nagayama, Langmuir **8**, 3183 (1992).

¹⁶P. Pieranski, L. Strzelecki, and B. Pansu, Phys. Rev. Lett. **50**, 900 (1983).

¹⁷S. G. Johnson and J. D. Joannopoulos, Opt. Express **8**, 173 (2001).

¹⁸H. Miguez, V. Kitaev, and G. A. Ozin, Appl. Phys. Lett. **84**, 1239 (2004).

¹⁹J. F. Galisteo-López and C. López, Phys. Rev. B **70**, 035108 (2004).

²⁰F. García-Santamaría, J. F. Galisteo-López, P. V. Braun, and C. López, Phys. Rev. B **71**, 195112 (2005).

²¹A. Blanco, H. Miguez, F. Meseguer, C. López, F. López-Tejiera, and J. Sánchez-Dehesa, Appl. Phys. Lett. **78**, 3181 (2001).

²²J. F. Bertone, P. Jiang, K. S. Hwang, D. M. Mittleman, and V. L. Colvin, Phys. Rev. Lett. **83**, 300 (1999).

²³J. F. Galisteo-López, E. Palacios-Lidón, E. Castillo-Martínez, and C. López, Phys. Rev. B **68**, 115109 (2003).